Effect of Ce doping on 2-nitrophenol adsorption at graphene surfaces

Saeedeh Ragabione, Saeedeh Hashemian*

Department of Chemistry, Islamic Azad University, Yazd Branch, Yazd, Iran, Tel. +09831872572; Fax: +0983517266065;
emails: Sa_hashemian@iauyazd.ac.ir (S. Hashemian), sragabion@yahoo.com (S. Ragabione)

ABSTRACT

Graphene and graphene doped with CeO_2 were prepared and characterized by FTIR, BET, XRD, SEM and elemental analysis. Adsorption of 2-nitrophenol by graphene and cerium doped graphene (CeO_2@ graphene nanocomposite) was studied. The impact of different parameters such as effect of adsorbent dosage, contact time and pH of solution were studied. Two common kinetic models, pseudo-first-order and pseudo-second- order were used to describe the adsorption kinetics. The resultant kinetic data were well fitted by a pseudo second-order model. Freundlich and Langmuir models were used to study the adsorption isotherms. Comparing with graphene, adsorption capacity of CeO_2@graphene toward 2-nitrophenol was enhanced significantly. The maximum adsorption capacity of graphene and CeO_2@graphene were determined 80.64 and 142 mg g^{-1}, respectively. Graphene and CeO_2@graphene had surface area of 27 and 95 m^2 g^{-1}, respectively. The thermodynamic results indicated the spontaneity and exothermic nature of the adsorption. CeO_2@graphene nanocomposite showed to be a highly efficient adsorbent and could be easily used for separation purposes.

Keywords: Adsorption; CeO_2@graphene; Doping; Nanocomposite; 2-nitrophenol

1. Introduction

Phenol products and nitroaromatic compounds are typical examples of wastewater pollutants. They are from a number of industrial processes including pharmaceutical, chemical, petrochemical, agricultural etc., [1]. Phenolic compounds are pollutants of great concern because of high toxicity and possible accumulation in the environment [2,3]. Phenolic compounds are in wastewaters from olivemill, oil refineries, plastics, leather, paint, pharmaceutical and steel industries, and must be removed to satisfy the actual environmental regulations. Nitroaromatic compounds also are used in many industrial processes, including preparation of pesticides, explosives, textiles, paper dyes, and other industrial chemicals. These compounds are often detected as water pollutants as a result of their release in industrial effluents [4]. Nitrophenols (NPs) are the most common organic pollutants in industrial and agricultural effluents. 4-nitrophenol is an important intermediate for the manufacture of analgesic and antipyretic drugs. As a result of the widespread applications, wastewaters and water resources, including groundwater and surface waters, have become contaminated with this compound. Different methods such as biodegradation, photocatalytic degradation [5], ozonation [6,7], decomposition by Fenton reagents [8] and oxidative degradation [9] were used to remove or eliminate phenolic compounds from polluted waters.

Adsorption process has proved as an effective technique for separation and removal of wide variety of pollutants from wastewater [10]. Adsorption has low initial cost, simplicity of design and ease of operation band insensitivity to toxic substances [11,12].

It has been found more preferred choice than other techniques for nitrophenol removal. Several adsorbents such as activated carbon [13], silica [14], polymeric resins [15] and zeolites [16] have all been proposed to remove phenolic pollutants from wastewater.

In most cases, the adsorbents have diameters in the range of submicron to micron and have large internal porosities to ensure adequate surface area for adsorption. However, the diffusion limitation within the particle leads to decreases in

* Corresponding author.

the adsorption rate and available capacity. Therefore, it is important and interesting to develop a novel adsorbent with a large surface area for adsorption, a small diffusion resistance and a high capacity.

Graphene, a single-atom-thick sheet of honey comb carbon lattice, exhibits many unique chemical and physical properties [17–19]. Since its discovery in 2004, extensive efforts have been devoted to investigating the technological applications of graphene materials, such as graphene-based electronics, high strength composite materials, liquid crystal displays, and energy storage and conversion devices [20–23]. Graphene oxide and different graphene based materials also were used as adsorbents [24].

The first aim of the present study is to synthesize and characterize graphene and CeO_2@graphene nanocomposite. Investigation of the efficiency of the graphene and CeO_2@ graphene nanocomposite as adsorbents for removal of 2-nitrophenol from aqueous solutions is the second goal. Through the second goal the effect of different variables including contact time and pH of solution was evaluated. The adsorption kinetic and thermodynamic studies of removal of 2-nitrophenol were also studied.

2. Experimental

2.1. Materials and methods

The all of chemicals were purchased from Merck chemical co. All of compounds were analytical grade and were used as received without any purification.

2-nitrophenol (1-hydroxy-2-nitrobenzene; CAS number: 88-75-5), with chemical formula of $HOC_6H_4NO_2$ as a sample of pollutant was used. It has molecular weight of 139.4 g mol^{-1}. The 2-nitrophenol standard solution of 1,000 mg L^{-1} was prepared and subsequently whenever necessary diluted. UV-Vis spectrophotometer 160A Shimadzu was used for determination of concentration of 2-nitrophenol. IR measurements were performed by FTIR tensor-27 of Burker Co., using the KBr pellet between the ranges 400–4,000 cm^{-1}. The powder X–ray diffraction studies were made on a Philips PW1840 diffractometer using Ni-filtered Cu k_α radiation and wavelength 1.54 Å. The average particle size and morphology of samples were observed by SEM using a Hitachi S-3500 scanning electron microscope. All pH measurements were carried out with an ISTEK- 720P pH meter. The surface area of the samples was determined using Brunauer–Emmett–Teller (BET) Quantachrome Autosorb-1 analyzer. CHN were analyzed by costech ECS-4010.

2.2. Preparation of graphene

Graphene was synthesized by the oxidation of graphite powder using Hummers method [24–26]. Firstly, 120 mL H_2SO_4 (95%) was added into a 500 mL flask, and then cooled by immersion in an ice bath followed by stirring. Subsequently, 5.0 g graphite powder and 2.5 g $NaNO_3$ were added under vigorous stirring to avoid agglomeration. After the graphite powder was well dispersed, 15 g $KMnO_4$ was added gradually under stirring and the temperature of the mixture was kept to be below 10°C by cooling. The ice bath was then removed and the mixture was stirred at room temperature overnight. As the reaction progressed, the

mixture gradually became pasty and the color turned into light brownish. Secondly, 150 mL of H_2O was slowly added to the paste with vigorous agitation. Because the addition of water in concentrated sulfuric acid medium released a large amount of heat, the addition of water was performed in an ice bath to keep the temperature below 100°C. The diluted suspension was stirred at 98°C for 1 d. Then, 50 mL of 30% H_2O_2 was added to the mixture. Finally, the mixture was filtered and washed with 5% HCl aqueous solution to remove metal ions followed by water until the pH was 7. After filtration and drying at 65°C under vacuum, graphene oxide was obtained as grey powder (named graphene in this study).

2.3. Preparation of CeO_2@graphene nanocomposite

0.1 g graphene prepared at section 2. 2 was dispersed in 100 mL H_2O and stirred over night to form a homogeneous aqueous dispersion. Then 100 mL aqueous solution of CeO_2 (0.355 g) was added into the graphene dispersion, and the obtained suspension was treated by ultrasonic treatment (600 W, 80% amplitude) for 1 h and followed by stirring at room temperature for 12 h. The suspension was separated by centrifugation, and the obtained residue was washed with deionized water for several times [23,24].

2.4. Adsorption experiments

Different parameters like: contact time, pH and effect of sorbent dosage on the sorption capacity of 2-nitrophenol have been studied. The removal of 2-nitrophenol from aqueous solutions by sorbents was carried out using following experimental procedures:

The initial 2-nitrophenol concentration in each sample was 40 mg L^{-1}. 0.1 g of sorbent was added in 30 ml sample on rotary shaker at a constant speed of 300 rpm. Samples were withdrawn at appropriate time intervals and centrifuged at 1,000 rpm for 5 min. All experiments were conducted at 25°C.

After different contact times (0–300 min), the sorbent was removed from the solution. Determination of 2-nitrophenol was done by different methods such as electrochemical synthesized Mg/Fe Layered double hydroxide sensor [27], multi-wall carbon nanotubes nafion-modified electrode [28] and spectrophotometric [29].

In this research the remaining concentration of the 2-nitrophenol in the solution was determined by spectrophotometric method by UV–vis spectrometry. The relative 2-nitrophenol adsorption (%) vs. adsorption time was determined. To optimize the adsorbent dosage, different doses of the sorbents was examined. A known amount of sorbent (0.05–1 g) was added to 30 mL of 2-nitrophenol solutions in the concentrations range from 20 to 60 mg L^{-1}. The influence of the solution pH on the 2-nitrophenol removal was also studied by adding a certain amount of the sorbent into the 2-nitrophenol solutions with the pH of the solution being adjusted from 2 to 10 with 0.1 mol L^{-1} HCl or 0.1 mol L^{-1} NaOH. The percent removal of 2-nitrophenol by the hereby adsorbent is given by:

$$\% \text{ Removal} = (C_0 - C_e)/C_0 \times 100 \tag{1}$$

where C_0, C_e is denoted the initial and equilibrium concentration (mg L^{-1}) of 2-nitrophenol, respectively. The removed

quantity (q_e in mg g^{-1}) of the 2-nitrophenol by sorbent was calculated:

$$q_e = (C_0 - C_e)V/m \qquad (2)$$

where C_0 (mg L^{-1}) represents the initial 2-nitrophenol concentration, C_e (mg L^{-1}) is the equilibrium concentration of the 2-nitrophenol remaining in the solution, V (L) is the volume of the aqueous solution, and m (g) is the weight of the sorbent.

3. Results and discussions

3.1. Characterization of graphene and CeO$_2$@ graphene

The FTIR spectra of graphene and CeO$_2$@graphene nanocomposite are shown in Figs. 1(A),(B). The FTIR spectra of graphene (Fig. 1(A)) shows broad band at 3,394 cm^{-1}, which is related to O-H stretching vibration. The band around 1,728 cm^{-1} is due to stretching vibrations from C=O. There are also bands due to carboxyl CO and C=C groups (1,728 and 1,618 cm^{-1}), and alkoxy C–O (1,047 cm^{-1}) groups situated at the edges of the graphene nano sheets, as previously reported [30,31]. The bond at 494 cm^{-1} (Fig. 1(B)), corresponding to a symmetrical stretching mode of vibrational unit Ce–O [32] and confirmed the formation of CeO$_2$@graphene.
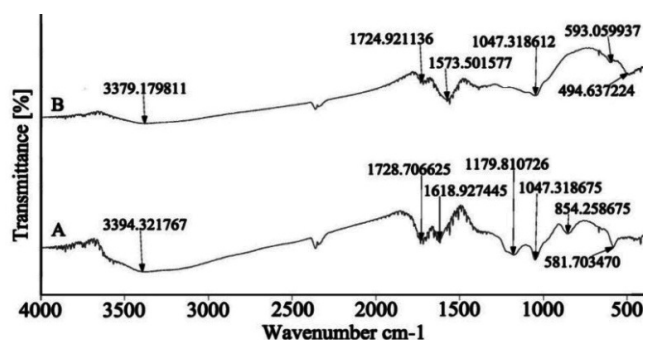

Fig. 1. FTIR pectra of (A)-graphene and (B)-CeO$_2$@graphene nanocomposite.
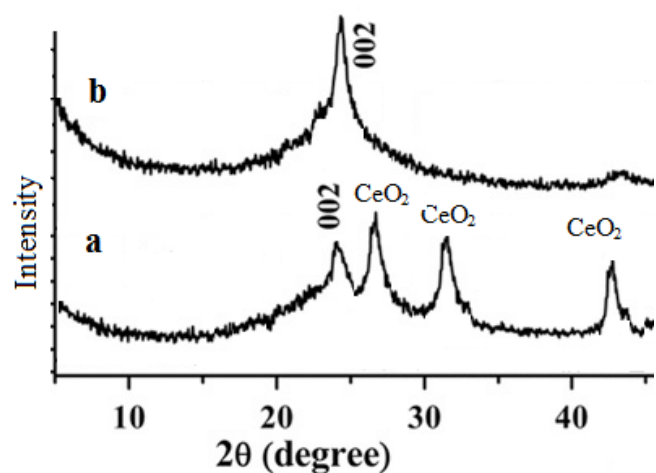

Fig. 2. XRD pattern of (a)-graphene and (b)-CeO$_2$@graphene.

XRD diffractometry of graphene and CeO$_2$@graphene composite are shown in Fig. 2. In graphene (Fig 2(a)), only one diffraction peak (002) could be found, which indicated the graphene structure with new oxygen containing groups were formed successfully by the strong oxidation reaction on the graphite. A broad (002) diffraction peak arising from the slight stacking of graphene nano sheets is also detected at a 2Θ of about 25° confirming the successful formation of graphene [33,34]. Fig. 2(b) shows the XRD patterns of CeO$_2$@graphene nanocomposite. In the composite, however, clear peaks of CeO$_2$ could be observed. The characteristic peaks, in good agreement with the standard data of CeO$_2$ (JCPDS No. 34-0394).

BET surface area analysis of graphene and CeO$_2$@graphene were investigated. Graphene and CeO$_2$@graphene had surface area of 27 and 95 m^2 g^{-1}, respectively.

CHN analyses of graphene and CeO$_2$@graphene are shown in Table 1.

The SEM images of graphene and CeO$_2$@graphene composite are shown in Figs. 3(a),(b). It can be clearly seen that the crumpled silk waves-likecarbon sheets exist, a characteristic feature of the single-layer graphene sheets (Fig. 3(a)). As shown in Fig. 3(b), the CeO$_2$ nanoparticles were successfully coated on the surface of graphene to form CeO$_2$@graphene. The average size of the CeO$_2$@graphene estimated from SEM observation was about 200 nm. The CeO$_2$ nanoparticles were well distributed on graphene sheets, which were nearly flat. SEM analysis showed that the composite is an aggregate of particles of CeO$_2$ anchored on graphene sheets and had big holes and porous. Therefore, SEM images confirmed the existence of pores on the surface of CeO$_2$@graphene. The CeO$_2$ particles are brighter on the graphene surface.

The results of energy-dispersive X-ray spectroscopy (EDX) recorded to investigate the elemental composition of graphene and CeO$_2$@graphene. The results demonstrate that mainly C and O appear in graphene. The EDX of CeO$_2$@graphene composite shows C, O and Ce, therefore, confirmed the formation of CeO$_2$@graphene nanocomposite. Fig. 4 shows the EDX of a-graphene and b-CeO$_2$@graphene

Table 1
CHN analysis of graphene and CeO$_2$@graphene composites

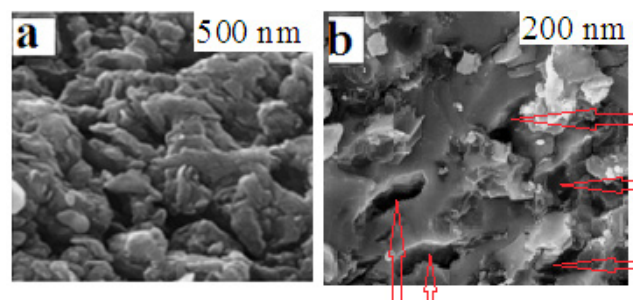| Sample	% C	% H	% N	% S
Graphene	81.6	1.12	0.20	14
CeO$_2$@graphene	47.2	0.82	0.07	12

Fig. 3. SEM image of (a)-graphene and (b)-CeO$_2$@graphene nanocomposite.

3.2. Adsorption study

3.2.1. Effect of contact time

The effect of the contact time on the removal of 2-nitrophenol by graphene and CeO$_2$@graphene was studied and the results are shown in Fig. 5. It is obvious from the Fig. 5 that increasing the contact time improved the adsorption process. This effect was especially observed within the first 15 min when most of the 2-nitrophenol was adsorbed. The percentage of 2-nitrophenol removal reached equilibrium within 15 min for CeO$_2$@graphene nanocomposite (with more than 90% removal) and 60 min for graphene (55% removal), respectively. It seems that the adsorption of 2-nitrophenol on CeO$_2$@graphene and graphene occurred in two consecutive steps. The first step, which is the faster, was transferred 2-nitrophenol molecules from the aqueous phase to the external surface of sorbents. The second slower step was the diffusion of the 2-nitrophenol molecules between the sorbents bundles. The adsorption of 2-nitrophenol by graphene was slower than CeO$_2$@graphene nanocomposite. The CeO$_2$ had catalytic effect on the graphene surface, and therefore, increased the adsorption capacity of graphene for 2-nitrophenol removal [36–38].
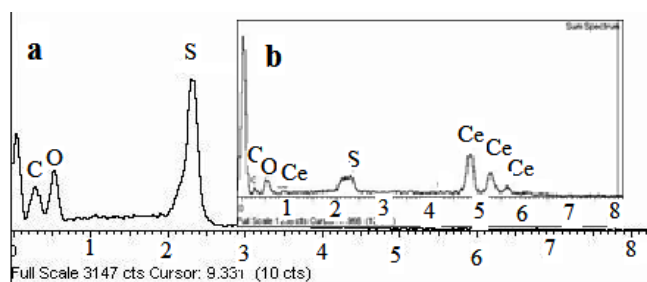
3.2.2. Effect of initial solution pH

Effect of pH of solution on the removal of 2-nitrophenol by graphene and CeO$_2$@graphene was studied. Using diluted solutions of hydrochloric acid and sodium hydroxide, the pHs were adjusted, and the results are presented in Fig. 6. At an acidic pH of 2.0, the percentage of 2-nitrophenol removal from aqueous solution was low. This low adsorption is primarily due to the electrostatic repulsion between the positively charged protonated graphene and the positively charged 2-nitrophenol molecules. Increasing the pH from 2.0 to 5.0 enhanced the percentage of 2-nitrophenol removal. At low pH most sorbent are positively charged, at least in part as a consequence of donor/acceptor interactions between the carbon graphene layers and the hydronium ions. The decreased surface acidity of graphene at pH > 5 favors the donor–acceptor interaction between the electrons of the aromatic ring and the surface. This leads to an increase of the removal efficiency [34,39].

3.2.3. Effect of adsorbent mass

The effect of sorbent dosage on the adsorption process was studied, and the results are illustrated in Fig. 7. It is clear

Fig. 4. EDX of (a)-graphene and (b)-CeO$_2$@graphene nanocomposite.

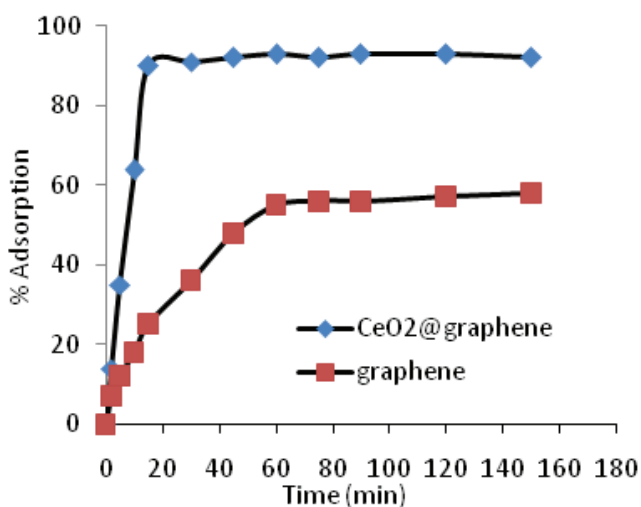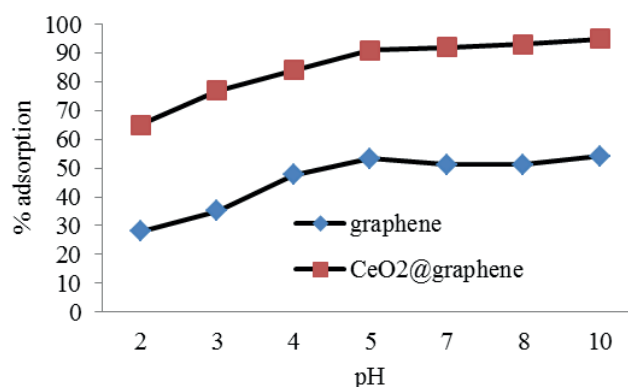Fig. 6. Effect of pH on the adsorption of 2-nitrophenol by graphene and CeO$_2$@graphene.

Fig. 5. Effect of the contact time on the adsorption of 2-nitrophenol by graphene and CeO$_2$@graphene (30 ml of 2-nitrophenol 40 mg L^{-1} and 30 mg sorbents).
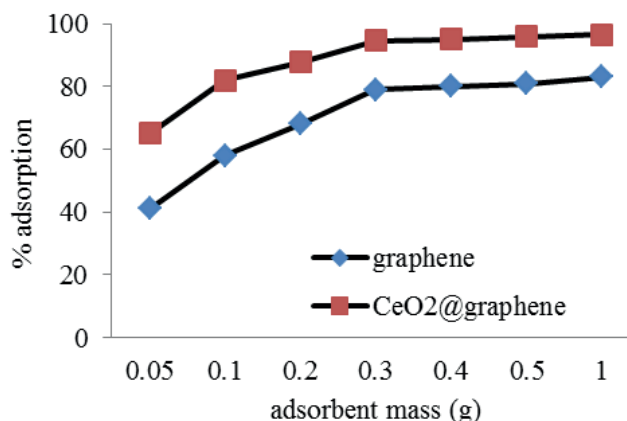

Fig. 7. Effect of adsorbent mass on the adsorption of 2-nitrophenol by graphene and CeO$_2$@graphene.

from Fig. 7 that the percentage of 2-nitrophenol removal from aqueous solution increased from 40% to 80% for graphene and 63% to 94% for CeO$_2$@graphene when the sorbent dose increased from 50 to 300 mg rapidly. But no significant adsorption was found beyond 300 to 1 mg. The increase in the percentage of 2-nitrophenol removal from aqueous solution is primarily due to the greater number of active sites available for adsorption as a result of the increased amount of sorbents. This observation may be due to the higher specific surface area of CeO$_2$@graphene. At CeO$_2$@graphene more than 300 mg, the incremental 2-nitrophenol removal is very small, because particle-particle interaction such as aggregation at higher mass of sorbent leads to a decrease in the availability of total surface area of the sorbent [40]. A dose of 300 mg of CeO$_2$@graphene was used for the further studies.

3.3. Adsorption kinetics

In other to analysis sorption kinetic data of 2-nitrophenol by graphene and CeO$_2$@graphene, two kinetic models, pseudo-first-order and pseudo-second-order models, were applied to establish the best fitted model for the experimental data. The linear equations of two models can be expressed as (Eq. (3)) for first-order and (Eq. (4)) second order

$$\ln(q_e - q_t) = \ln q_e - k_1 t \tag{3}$$

$$t/q_t = 1/(k_2 q_e^2) + t/q_e \tag{4}$$

where is q_t adsorbed at equilibrium and at time t (min), respectively. k_1 (min^{-1}) and k_2 (g mg^{-1} min^{-1}) are rate constants of the first order and second order adsorption, respectively.

Values of k_1 and q_e can be calculated from the slope and intercept of the plots of $\ln(q_e - q_t)$ vs. t for Eq. (3) and values of q_e and k_2 can be obtained from the linear plots of t/q_t against t for Eq. (4). Table 1 exhibits the adsorption kinetic parameters of 2-nitrophenol onto graphene and CeO$_2$@graphene nanocomposite. From Table 2, considering the higher values of R^2 and lower deviation between experimental and calculated q_e values, the adsorption of 2-nitrophenol onto graphene and CeO$_2$@graphene nanocomposite both obeyed pseudo-second-order kinetic model (Fig. 8). It could be concluded chemical interaction might be involved in the adsorption process [37].

3.4. Adsorption isotherm

The quantity of 2-nitrophenol that could be adsorbed over the surface of sorbent, is a function of concentration and may be explained by adsorption isotherms. Adsorption isotherm models of Langmuir and Freundlich were employed to describe experimental adsorption data. The Langmuir isotherm is based on assumption of that the adsorption process take place on homogenous adsorbent surfaces with constant energy, whiles Freundlich isotherm assuming that the adsorption process occurs on heterogeneous surfaces with non-uniform distribution of adsorption heat. The Freundlich adsorption isotherm model can be represented as follows:
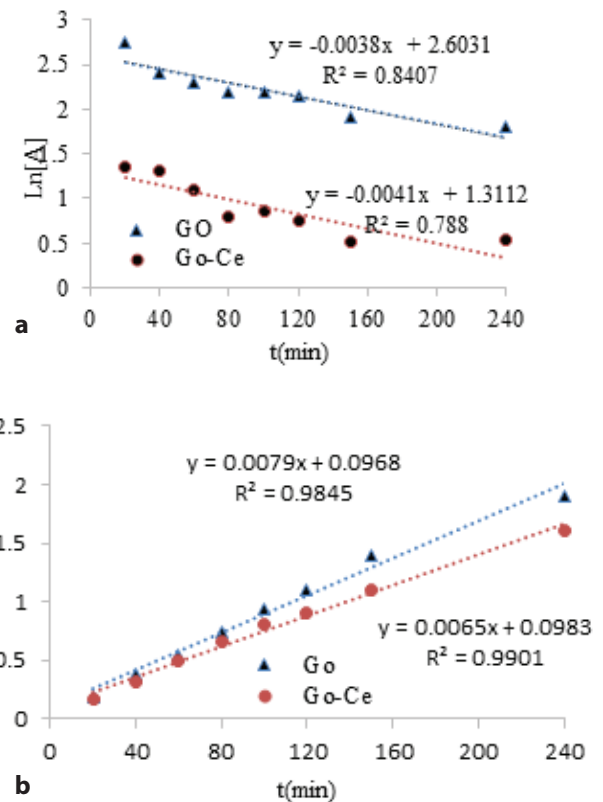
$$q_e = K_F C_e^{1/n} \tag{5}$$

Fig. 8. The kinetic models for 2-nitrophenol adsorption on graphene and CeO$_2$@graphene, (a) Pseudo-first order, (b) Pseudo-second order.

Table 2
Kinetic parameters for adsorption of 2-nitrophenol onto graphene and CeO$_2$@graphene

Sorbents	First order		Second order	
	R^2	K_1 (min^{-1})	R^2	K_2 (g mg^{-1} min^{-1})
Graphene	0.84	3×10^{-3}	0.984	1.317
CeO$_2$@graphene	0.788	4×10^{-3}	0.990	1.54

In most references, Freundlich adsorption may also be expressed as the following equation:

$$\log q_e = \log K_F + 1/n \log C_e \tag{6}$$

The Langmuir adsorption model is given as:

$$C_e/q_e = C_e/K_L q_m + C_e/q_m \tag{7}$$

where q_e is the solid phase equilibrium concentration (mg g^{-1}), C_e is the liquid equilibrium concentration of 2-nitrophenol in solution (mg L^{-1}), K_F is the Freundlich constant representing the adsorption capacity (mg g^{-1}), and n is the heterogeneity factor depicting the adsorption intensity, K_L is the equilibrium adsorption constant related to the affinity of binding sites (L mg^{-1}), and q_m is the maximum amount of 2-nitrophenol per unit weight of adsorbent for complete monolayer

Table 3
Langmuir and Freundlich constants for the adsorption of 2-nitrophenol onto graphene and CeO_2@graphene

Sorbent	Freundlich			Langmuir		
	K_F mg g^{-1}	n	R^2	q_m mg g^{-1}	K_L L mg^{-1}	R^2
Graphene	0.175	0.97	0.927	80.64	0.22	0.985
CeO_2@graphene	0.114	1.24	0.933	142	0.438	0.998

coverage (mg g^{-1}). The isotherm parameters of Langmuir and Freundlich for adsorption of 2-nitrophenol onto graphene and CeO_2@graphene are listed in Table 3. It is evident from Table 3 that the equilibrium data were better represented by Langmuir isotherm equation than by the Freundlich equation [38]. It is known that the Langmuir isotherm is used on the supposition that the surface of the adsorbent is a homogenous surface, whereas the Freundlich isotherm applies to the adsorption process on a heterogeneous surface.

3.5. Thermodynamic studies

In order to thermodynamic study of the adsorption process, determination of the main three parameters requires. These parameters included: the standard enthalpy ΔH°, the standard free energy ΔG° and the standard entropy ΔS°. The amounts of ΔH° and ΔS° calculated using from the intercept and slope of vant' Hoff plots of lnK_C vs. 1/T (Eq. 9), respectively and the following equation:

$$K_C = q_e/C_e \tag{8}$$

$$\ln K_C = -\Delta H°/RT + \Delta S°/R \tag{9}$$

$$\Delta G° = -RT \ln K_C \tag{10}$$

where K_C (L g^{-1}) is the distribution coefficient, q_e and C_e are the amount of 2-nitrophenol adsorbed at equilibrium (mg g^{-1}) and equilibrium concentration in solution (mg L^{-1}), respectively. ΔG° is the standard free energy change, T the absolute temperature and R the universal gas constant (8.314 J mol^{-1} K^{-1}). ΔH° and ΔS° were calculated the slope and intercept of van't Hoff plots of ln K_C vs. 1/T (Fig. 9). The results of thermodynamic parameters of adsorption of 2-nitrophenol onto graphene and CeO_2@graphene are given in Table. 4. The negative amounts of ΔH° and ΔG° show that the adsorption process of 2-nitrophenol by graphene and CeO_2@graphene is exothermic and spontaneous. The overall standard free energy change during the adsorption process was negative for the experimental range of temperatures and the system did not gain energy from an external source. It becomes more favorable when temperature increased [39].

3.6. Comparison of CeO_2@graphene nanocomposite with other adsorbents

The adsorption capacity of 2-nitrophenol onto CeO_2@ graphene nanocomposite was compared with several other adsorbents and they are reported in Tables 4 and 5. CeO_2@ graphene nano composites in this study possess reasonable adsorption capacity in comparison with other sorbents.
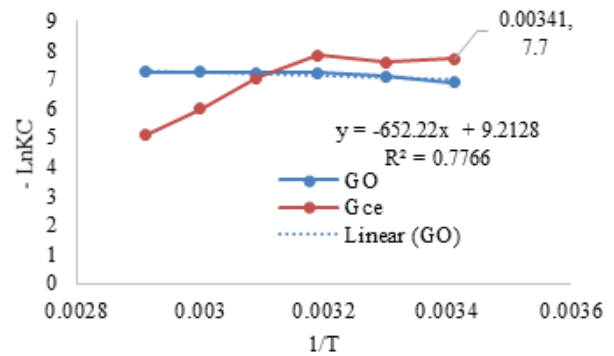

Fig. 9. Plot of lnK_c vs. 1/T.

Table 4
Thermodynamic parameters for adsorption of 2-nitrophenol onto graphene and CeO_2@graphene

Sorbent	ΔG° (KJ mol^{-1})	T (K)	ΔH° (J mol^{-1})	ΔS° (J mol^{-1}K^{-1})
Graphene	−16.8	293	−0.2826	
	−17.88	303		60.79
	−18.78	313		
	−19.41	323		
	−20.04	333		
	−20.07	343		
CeO_2@graphene	−18.32	293	−6.816	
	−19.06	303		40.17
	−20.34	313		
	−18.91	323		
	−15.4	333		
	−14.53	343		

4. Conclusion

Graphene and CeO_2@graphene nanocomposite was successfully prepared.

Graphene and CeO_2@graphene composite were characterized by FTIR, XRD, BET, elemental analysis and SEM. Adsorption of 2-nitrophenol by CeO_2@graphene nanocomposite was done at contact time of 30 min and pH > 5. Experimental results demonstrated CeO_2@graphene nanocomposite had higher efficiency and faster rate for adsorption of 2-nitrophenol than graphene. Kinetic data indicated the adsorption of 2-nitrophenol by graphene and CeO_2@ graphene was followed by pseudo-second order kinetic model. Kinetic of adsorption of 2-nitrophenol by CeO_2@ graphene was occurred in two steps. Equilibrium studies of 2-nitrophenol removal by CeO_2@graphene nanocomposite indicated adsorption was fit with Langmuir isotherm model. The facile synthetic conditions, efficient and fast adsorption process, as well as simple separation process offered the adsorbent potential use in removal of nitrophenol. This information may be useful for further research and practical applications of novel graphene and CeO_2@ graphene adsorbent in nitrophenols wastewater treatment.

Table 5
Comparison of maximum adsorption capacities of 2-nitrophenol with different sorbents

Adsorbent	Isotherm model	Kinetic model	q_m (mg g^{-1})	Pollutant	Refs.
zeolite	Langmuir	2°	12.7	4-nitrophenol	[40]
bentonite	Langmuir	2°	15.19	4-nitrophenol	[40]
Sawdust	Langmuir	–	15.3	4-nitrophenol	[41]
SWCNTs	Langmuir	–	1.444	4-chloro-2-nitrophenol	[11]
MWCNTs	Langmuir	–	4.426	4-chloro-2-nitrophenol	[11]
nZVI	Langmuir	2°	4.8476	4-chloro-2-nitrophenol	[42]
Pd-nZVI	Langmuir	2°	6.6181	4-chloro-2-nitrophenol	[42]
Graphene oxide	Langmuir	2°	80.64	2-nitrophenol	Present study
CeO$_2$@graphene	Langmuir	2°	142	2-nitrophenol	Present study

Acknowledgements

References

[1] S. Chen, Z.P. Xu, O. Zhang, G.Q. Lu, Z.P. Hao, S. Liu, Studies on adsorption of phenol and 4-nitrophenol on MgAl-mixed oxide derived from MgAl-layered double hydroxide, Sep. Purif. Technol., 67 (2009) 194–200.

[2] Y. Ku, K.C. Lee, Removal of phenols from aqueous solution by XAD-4 resin, J. Hazard. Mater., B80 (2000) 59–68.

[3] Z. Aksu, J. Yener, A comparative adsorption/biosorption study of mono-chlorinated phenols onto various sorbents, Waste Manage., 21 (2001) 695–702.

[4] M. Carmona, A. De Lucas, J.L. Valverde, B. Velasco, J.F. Rodriguez, Combined adsorption and ion exchange equilibrium of phenol on Amberlite IRA-420, Chem. Eng. J., 117 (2006) 155–160.

[5] J. Sarasa, M.P. Roche, M.P. Ormad, E. Gimeno, A. Puig, J.L. Ovelleiro, Treatment of a wastewater resulting from dyes manufacturing with ozone and chemical coagulation, Water Res., 32 (1998) 2721–2727.

[6] G.R. Soltanian, M. Havaee Behbahani, The effect of metal oxides on the refinery effluent treatment, Iran, J. Environ. Health Sci. Eng., 8 (2011) 169–174.

[7] F.J. Benitez, J. Beltran-Heredia, J.L. Acero, F.J. Rubio, Rate constants for the reactions of ozone with chlorophenols in aqueous solutions, J. Hazard. Mater. B, 79 (2000) 271–285.

[8] P. Gharbani, M. Khosravi, S.M. Tabatabaii, K. Zare, S. Dastmalchi, A. Mehrizad, Degradation of trace aqueous 4-chloro-2-nitrophenol occurring inpharmaceutical industrial wastewater by ozone, Int. J. Environ. Sci. Technol., 7 (2010) 377–384.

[9] M. Farrokhi, A.R. Mesdaghinia, A.R. Yazdanbakhsh, S. Nasseri, Characteristics of Fenton's oxidation of 2, 4, 6 trichlorophenol, Iran, J. Environ. Health Sci. Eng., 1 (2004) 12–18.

[10] J. Beunink, H.J. Rehm, Coupled reductive and oxidative degradation of 4-chloro-2-nitrophenol by a co-immobilized mixed culture system, Appl. Microbiol. Biotechnol., 34 (1990) 108–115.

[11] A. Mehrizad, M. Aghaie, P. Gharbani, S. Dastmalchi, M. Monajjemi, K. Zare, Comparison of 4-chloro-2-nitrophenol adsorption on single-walled and multi-walled carbon nanotubes, Iran, J. Environ. Health Sci. Eng., 9 (2012) 5–9.

[12] A. Mehrizad, K. Zare, H. DashtiKhvidaki, S. Dastmalchi, H. Aghaie, P. Gharbani, Kinetic and thermodynamic studies of adsorption of 4-chloro-2-nitrophenol on nano-TiO$_2$, J. Phys. Theor. Chem., 8 (2011) 33–37.

[13] R.L. Tseng, K.T. Wu, F.C. Wu, R.S. Juang: kinetic studies on the adsorption of phenol, 4-chlorophenol, and 2, 4-dichlorophenol from water using activated carbons, J. Environ. Manage., 91 (2010) 2208–2214.

[14] N. Roostaei, F.H. Tezel, Removal of phenol from aqueous solutions by adsorption, J. Environ. Manage., 70 (2004) 157–164.

[15] K. Abburi, Adsorption of phenol and p-chlorophenol from their single and bisolute aqueous solutions on Amberlite XAD-16 resin, J. Hazard. Mater., 105 (2003) 143–156.

[16] S. Koh, J.B. Dixon, Preparation and application of organo minerals as adsorbents of phenol, benzene and toluene, Appl. Clay Sci., 18 (2001) 111–122.

[17] K.S. Novoselov, A.K. Geim, S.V. Morozov, D. Jiang, Y. Zhang, S.V. Dubonons, I.V. Grigorieva, A.A. Firsov, Electric field effect in atomically thin carbon films, Science, 306 (2004) 666–669.

[18] K.S. Novoselov, A.K. Geim, S.V. Morozov, D. Jiang, M.I. Katsnelson, I.V. Grigorieva, S.V. Dubonons, A.A. Firsov, Two-dimensional gas of massless Dirac fermions in graphene, Nature, 438 (2005) 197–200.

[19] C. Berger, Z.M. Song, X.B. Li, X.S. Wu, N. Brown, C. Naud, D. Mayou, T.B. Li, J. Hass, A.N. Marchenkov, E.H. Conrad, P.N. First, W.A. de Heer, Electronic confinement and coherence in patterned epitaxial graphene, Science, 312 (2006) 1191–1196.

[20] X. Wang, L.J. Zhi, K. Müllen, Transparent, Conductive graphene electrodes for dye-sensitized solar cells, Nano Lett., 8 (2008) 323–327.

[21] S. Stankovich, D.A. Dikin, G.H.B. Dommett, K.M. Kohlhaas, E.J. Zimney, E.A. Stach, R.D. Piner, S.T. Nguyen, R.S. Ruoff, Graphene-based composite materials, Nature, 442 (2006) 282–286.

[22] M.D. Stroller, S. Park, Y. Zhu, J. An, R.S. Ruoff, Graphene-based ultracapacitors, Nano Lett., 8 (2008) 3498–3502.

[23] Z. Du, X. Yin, M. Zhang, Q. Hao, Y. Wang, T. Wang, In situ synthesis of SnO$_2$/graphene nanocomposite and their application as anode material for lithium ion battery, Mater. Lett., 64 (2010) 2076–2079.

[24] S. Hashemian, M. Rahimi, A.A. Kerdegari, CuFe$_2$O$_4$@graphene nanocomposite as a sorbent for removal of alizarine yellow azo dye from aqueous solutions, Desal. Wat. Treat., 57 (2016) 14696–14707.

[25] W.S. Hummers, R.E. Offeman, Preparation of graphitic oxide, J. Am. Chem. Soc., 80 (1958) 1339.

[26] X. Yang, X. Zhang, Y. Ma, Y. Huang, Y. Wang, Y. Chen, Super paramagnetic graphene oxide-Fe$_3$O$_4$ nanoparticles hybrid for controlled targeted drug carriers, J. Mat. Chem., 19 (2009) 2710–2714.

[27] K. Nejati, K. Asadpour-Zeynali, Z. Rezvani, R. Peyghami, Determination of 2-nitrophenol by electrochemical synthesized Mg/Fe layered double hydroxide sensor, Int. J. Electrochem. Sci., 9 (2014) 5222–5234.

[28] W. Huang, C. Yang, S. Zhang, Simultaneous determination of 2-nitrophenol and 4-nitrophenol based on the multi-wall carbon nanotubes nafion-modified electrode, Anal. Bioanal. Chem., 375 (2003) 703–707.

[29] F. Bagheban-Shahri, A. Niazi, A. Akrami, Simultaneous spectrophotometric determination of nitrophenol isomers in environmental samples using first derivative of the density ratio spectra, J. Chem. Health Risks, 2 (2012) 21–28.

[30] D. Li, M.B. Muller, S. Gilje, R.B. Kaner, G.G. Wallace, Processable aqueous dispersions of graphenenanosheets, Nat. Nanotechnol., 3 (2008) 101–105.

[31] C. Wang, C. Feng, Y. Gao, X. Ma, Q. Wu, Z. Wang, Preparation of a graphene-based magnetic nanocomposite for the removal of an organic dye from aqueous solution, Chem. Eng. J., 173 (2011) 92–97.

[32] M.F. Pinheiro da Silva, L.S. Soeira, K.R.P. Dagasthanli, T.S. Martins, I.M. Cucovia, R.S. Freire, P.C. Isolani, CeO_2-catalyzed ozonation of phenol: the role of cerium citrate as precursor of CeO_2, J. Therm. Anal. Calorim., 102 (2010) 907–913.

[33] M.F. Pinheiro da Silva, H.C.d.J. Fraga da Costa, E.R. Triboni, M.J. Politi, P.C. Isolani, Synthesis and characterization of CeO_2–graphene composite, J. Therm. Anal. Calorim., 107 (2012) 257–263.

[34] Z. Ji, X. Shen, M. Li, H. Zhou, G. Zhu, K. Chen, Synthesis of reduced graphene oxide/CeO_2 nanocomposites and their photo catalytic properties, Nanotechnology, 24 (2013) 115603–115612.

[35] H. Jeong, Y.P. Lee, R.J.W.E. Lahaye, M. Park, K.H. An, I.J. Kim, C. Yang, C.Y. Park, R.S. Ruoff, Y.H. Lee, Evidence of graphitic and stacking order of graphite oxides, J. Am. Chem. Soc., 130 (2008) 1362–1366.

[36] Z.F. Liu, Q. Liu, Y. Huang, Y.F. Ma, S.G. Yin, X.Y. Zhang, W. Sun, Y.S. Chen, Organic photovoltaic devices based on a novel acceptor material: graphene, Adv. Mater., 20 (2008) 3924–3930.

[37] H. Zhang, X.J. Lv, Y. M. Li, Y. Wang, J.H. Li, P25-graphene composite as a high performance photocatalyst, ACS Nano, 4 (2010) 380–386.

[38] L. Jiang, M. Yao, B. Liu, Q. Li, R. Liu, H. Lv, S. Lu, C. Gong, B. Zou, T. Cui, B. Liu, G. Hu, T. Wagberg, Controlled synthesis of CeO_2/graphene nanocomposites with highly enhanced optical and catalytic properties, J. Phys. Chem. C, 116 (2012) 11741–11745.

[39] M. Zhang, R. Yuan, Y. Chai, C. Wang, X. Wu, Cerium oxide–graphene as the matrix for cholesterol sensor, Anal. Biochem., 436 (2013) 69–74.

[40] S. Hashemian, M. Mirshamsi, Kinetic and thermodynamic of adsorption of 2-picoline by sawdust from aqueous solution, J. Ind. Eng. Chem., 18 (2012) 2010–2015.

[41] Y.P. Chang, C.L. Ren, J.C. Quc, X.G. Chen, Preparation and characterization of Fe_3O_4/graphene nano composite and investigation of its adsorption performance for aniline and p-chloroaniline, Appl. Surface Sci., 261 (2012) 504–509.

[42] S. Hashemian, A. Foroghimoqhadam, Effect of copper doping on $CoTiO_3$ Ilmenite type nano particles for removal of congo red from aqueous solution, Chem. Eng. J., 235 (2014) 299–306.

[43] G. Varank, A. Demir, K. Yetilmezsoy, S. Top, E. Sekman, M. Bilgili, Removal of 4-nitrophenol from aqueous solution by natural low-cost adsorbents, Indian J. Chem. Technol., 19 (2012) 7–25.

[44] A.E. Ofomaja, E.I. Unuabonah, Kinetics and time-dependent Langmuir modeling of 4-nitrophenol adsorption onto Mansonia sawdust, J. Taiwan Ins. Chem. Eng., 44 (2013) 566–576.

[45] S. Adami, A. Fakhri, Adsorption of 4-chloro-2-nitrophenol by zero valent iron nanoparticles and pd-doped zero valent iron nanoparticles surfaces: isotherm, kinetic and mechanism modeling, Phys. Chem. Biophys., 3 (2013) 1–5.